Anisotropy of acoustooptic figure of merit for TeO₂ crystals. 2. Anisotropic diffraction: Errata

Mys O., Kostyrko M., Zapeka B., Krupych O. and Vlokh R.

Vlokh Institute of Physical Optics, 23 Dragomanov Street, 79005 Lviv, Ukraine, vlokh@ifo.lviv.ua

Abstract. We address the errors found in our recent analysis of anisotropy of the acoustooptic figure of merit in TeO₂ crystals [Mys O. et al., 2015. Ukr. J. Phys. Opt. **16**: 38–60].

We have found some errors in our recent analysis of anisotropy of acoustooptic figure of merit (AOFM) performed in Ref. [1] for the case of anisotropic acoustooptic (AO) diffraction in TeO₂ crystals. These errors are caused by the fact that we have not taken into account the changes in polarization of the diffracted optical wave due to changing orientation of the interaction plane that occurs under its rotation around the principal axes X and Z and due to changing diffraction angle. As a result, Eqs.(8)–(11) and the relation $E = \sqrt{E_1^2 + E_2^2 + E_3^2}$ in Ref. [1] are incorrect. The correct electric field of the diffracted optical wave in the case of diffraction occurring in the interaction plane XZ rotated around the X and Z axes by the angle φ_X and φ_Z is as follows:

$$E = E_1 \frac{\sin(\theta + \gamma)\sin\varphi_X}{\sqrt{\cos^2(\theta + \gamma) + \sin^2(\theta + \gamma)\sin^2\varphi_X}} - E_2 \frac{\cos(\theta + \gamma)}{\sqrt{\cos^2(\theta + \gamma) + \sin^2(\theta + \gamma)\sin^2\varphi_X}}, \quad (1)$$

$$E = E_2 \cos\varphi_Z - E_1 \sin\varphi_Z. \quad (2)$$

Here E_1 and E_2 are the electric field components of the diffracted wave, and θ and γ the angles of the incident and diffracted waves with respect to the axes X and X', respectively. Then the relations for the effective elastooptic coefficients (EECs) for the interaction types (VII)–(IX), Eqs. (24)–(29) in Ref. [1], should be corrected as follows:

$$p_{ef}^{(VII)} = \left\{ \begin{matrix} \left[p_{11}\cos^2\chi\cos^2\varphi_Z + p_{12}\cos^2\chi\sin^2\varphi_Z + p_{13}\sin^2\chi \right]\sin\theta\cos\varphi_Z \\ + p_{66}\cos^2\chi\sin2\varphi_Z\sin\theta\sin\varphi_Z + p_{44}\sin2\chi\cos\varphi_Z\cos\theta \end{matrix} \right\}\sin\varphi_Z$$

$$- \left\{ \begin{matrix} p_{66}\cos^2\chi\sin2\varphi_Z\sin\theta\cos\varphi_Z \\ + \left[p_{12}\cos^2\chi\cos^2\varphi_Z + p_{11}\cos^2\chi\sin^2\varphi_Z + p_{13}\sin^2\chi \right]\sin\theta\sin\varphi_Z \\ + p_{44}\sin2\chi\sin\varphi_Z\cos\theta \end{matrix} \right\}\cos\varphi_Z \quad , \quad (3)$$

$$p_{ef}^{(VII)} = \left\{ \begin{array}{l} \left[p_{11}\cos^2\chi + p_{12}\sin^2\chi\sin^2\varphi_X + p_{13}\sin^2\chi\cos^2\varphi_X \right]\dfrac{0.5\sin 2\theta\cos\varphi_X}{\sqrt{1-\sin^2\theta\cos^2\varphi_X}} \\[3mm] -p_{66}\sin 2\chi\sin\varphi_X\dfrac{0.5\sin^2\theta\sin 2\varphi_X}{\sqrt{1-\sin^2\theta\cos^2\varphi_X}} + p_{44}\sin 2\chi\cos\varphi_X\sqrt{1-\sin^2\theta\cos^2\varphi_X} \end{array} \right\}$$

$$\times\frac{\sin(\theta+\gamma)\sin\varphi_X}{\sqrt{\cos^2(\theta+\gamma)+\sin^2(\theta+\gamma)\sin^2\varphi_X}}$$

$$-\left\{ \begin{array}{l} -p_{66}\sin 2\chi\sin\varphi_X\dfrac{0.5\sin 2\theta\cos\varphi_X}{\sqrt{1-\sin^2\theta\cos^2\varphi_X}} \\[3mm] +\left[p_{12}\cos^2\chi + p_{11}\sin^2\chi\sin^2\varphi_X + p_{13}\sin^2\chi\cos^2\varphi_X \right]\dfrac{0.5\sin^2\theta\sin 2\varphi_X}{\sqrt{1-\sin^2\theta\cos^2\varphi_X}} \\[3mm] -p_{44}\sin^2\chi\sin 2\varphi_X\sqrt{1-\sin^2\theta\cos^2\varphi_X} \end{array} \right\} \qquad , \quad (4)$$

$$\times\frac{\cos(\theta+\gamma)}{\sqrt{\cos^2(\theta+\gamma)+\sin^2(\theta+\gamma)\sin^2\varphi_X}}$$

$$p_{ef}^{(VIII)} = \left\{ \begin{array}{l} 0.5\left[(p_{13} - p_{11}\cos^2\varphi_Z - p_{12}\sin^2\varphi_Z)\sin 2\chi \right]\sin\theta\sin\varphi_Z \\[2mm] -0.5p_{66}\sin 2\chi\sin 2\varphi_Z\sin\theta\cos\varphi_Z + p_{44}\cos 2\chi\cos\varphi_Z\cos\theta \end{array} \right\}\sin\varphi_Z$$

$$, \quad (5)$$

$$+\left\{ \begin{array}{l} 0.5p_{66}\sin 2\chi\sin 2\varphi_Z\sin\theta\sin\varphi_Z \\[2mm] +\left[p_{12}\cos^2\varphi_Z + p_{11}\sin^2\varphi_Z - p_{13} \right]\sin 2\chi\,0.5\sin\theta\cos\varphi_Z \\[2mm] +p_{44}\cos 2\chi\sin\varphi_Z\cos\theta \end{array} \right\}\cos\varphi_Z$$

$$p_{ef}^{(VIII)} = \left\{ \begin{array}{l} 0.25\left[p_{12}\sin^2\varphi_X + p_{13}\cos^2\varphi_X - p_{11} \right]\sin 2\chi\dfrac{\sin 2\theta\cos\varphi_X}{\sqrt{1-\sin^2\theta\cos^2\varphi_X}} \\[3mm] -p_{66}\sin\varphi_X\cos 2\chi\dfrac{0.5\sin^2\theta\sin 2\varphi_X}{\sqrt{1-\sin^2\theta\cos^2\varphi_X}} \\[3mm] +p_{44}\cos\varphi_X\cos 2\chi\sqrt{1-\sin^2\theta\cos^2\varphi_X} \end{array} \right\}$$
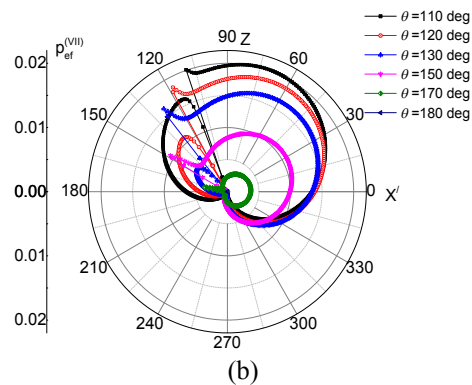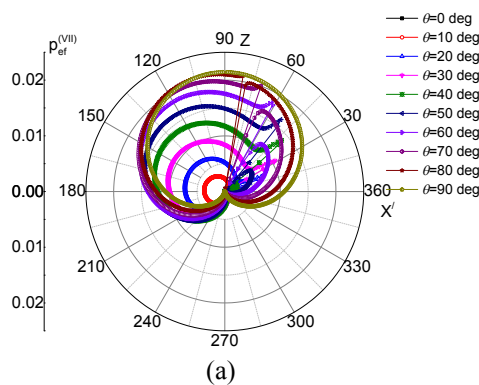
$$\times\frac{\sin(\theta+\gamma)\sin\varphi_X}{\sqrt{\cos^2(\theta+\gamma)+\sin^2(\theta+\gamma)\sin^2\varphi_X}} \qquad (6)$$

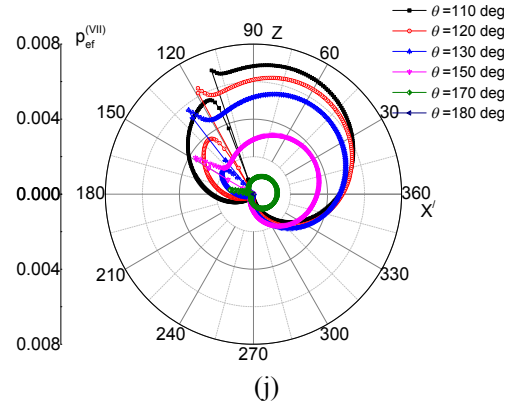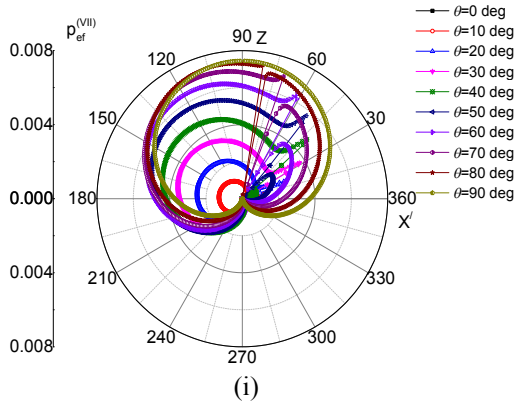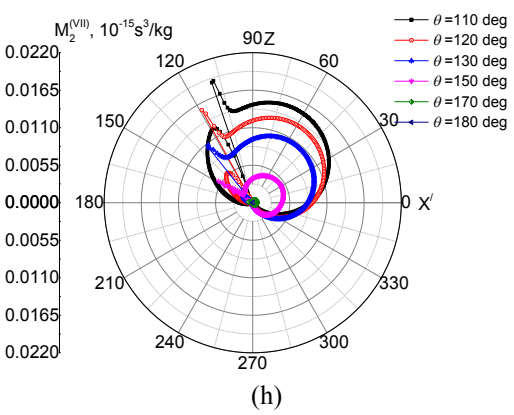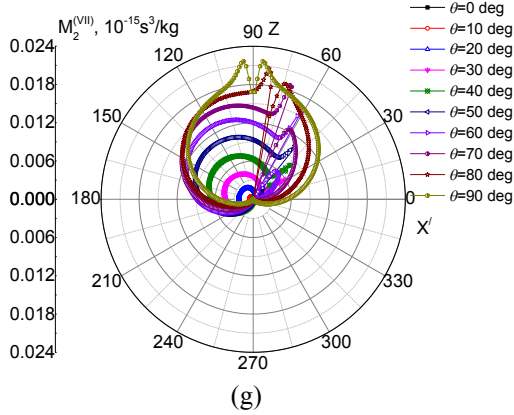$$+\left\{ \begin{array}{l} p_{66}\sin\varphi_X\cos 2\chi\dfrac{0.5\sin 2\theta\cos\varphi_X}{\sqrt{1-\sin^2\theta\cos^2\varphi_X}} \\[3mm] +0.25\left[p_{12} - p_{11}\sin^2\varphi_X - p_{13}\cos^2\varphi_X \right]\sin 2\chi\dfrac{\sin^2\theta\sin 2\varphi_X}{\sqrt{1-\sin^2\theta\cos^2\varphi_X}} \\[3mm] -0.5p_{44}\sin 2\varphi_X\sin 2\chi\sqrt{1-\sin^2\theta\cos^2\varphi_X} \end{array} \right\}$$

$$\times\frac{\cos(\theta+\gamma)}{\sqrt{\cos^2(\theta+\gamma)+\sin^2(\theta+\gamma)\sin^2\varphi_X}}$$

$$p_{ef}^{(IX)} = \left\{ \begin{array}{l} 0.5(p_{11} - p_{12})\cos\chi\sin 2\varphi_Z \sin\theta\sin\varphi_Z + \\ + p_{66}\cos\chi\cos 2\varphi_Z \sin\theta\cos\varphi_Z + p_{44}\sin\chi\sin\varphi_Z\cos\theta \end{array} \right\} \sin\varphi_Z$$

,   (7)

$$- \left\{ \begin{array}{l} p_{66}\cos\chi\cos 2\varphi_Z \sin\theta\sin\varphi_Z \\ -(p_{11} - p_{12})0.5\cos\chi\sin 2\varphi_Z \sin\theta\cos\varphi_Z \\ -p_{44}\sin\chi\cos\varphi_Z\cos\theta \end{array} \right\} \cos\varphi_Z$$

$$p_{ef}^{(IX)} = \left\{ \begin{array}{l} 0.25(p_{12} - p_{13})\sin\chi\sin 2\varphi_X \dfrac{\sin 2\theta\cos\varphi_X}{\sqrt{1 - \sin^2\theta\cos^2\varphi_X}} \\ + 0.5 p_{66}\cos\varphi_X \cos\chi \dfrac{\sin^2\theta\sin 2\varphi_X}{\sqrt{1 - \sin^2\theta\cos^2\varphi_X}} + \\ + p_{44}\sin\varphi_X \cos\chi\sqrt{1 - \sin^2\theta\cos^2\varphi_X} \end{array} \right\}$$

$$\times \frac{\sin(\theta + \gamma)\sin\varphi_X}{\sqrt{\cos^2(\theta + \gamma) + \sin^2(\theta + \gamma)\sin^2\varphi_X}}$$
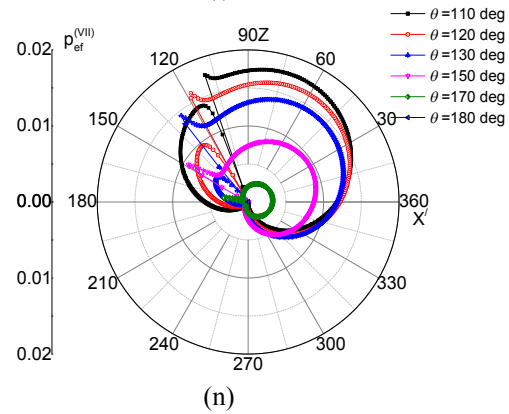
(8)
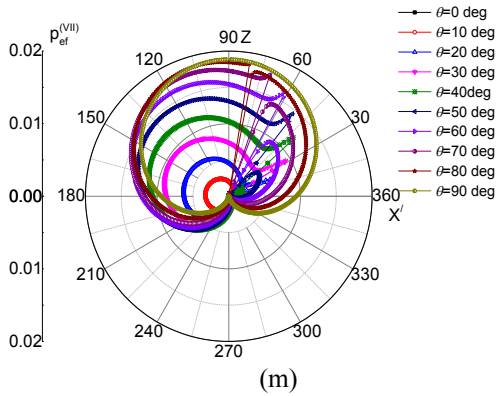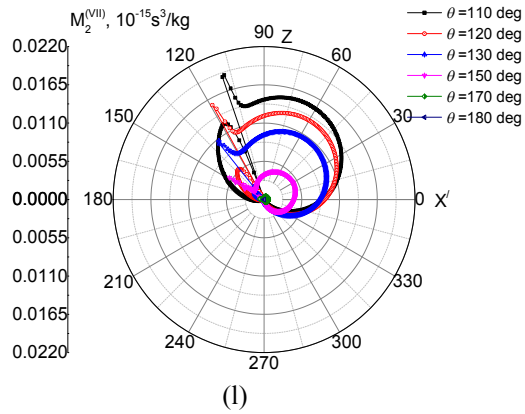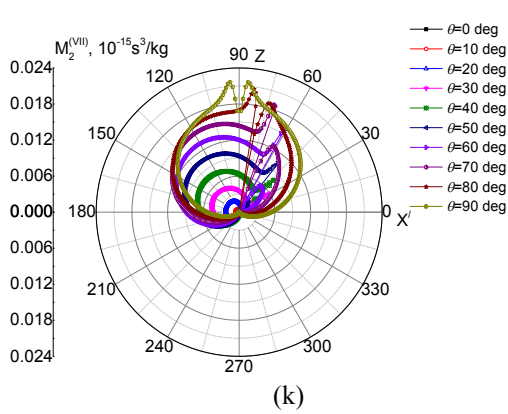
$$- \left\{ \begin{array}{l} 0.5 p_{66}\cos\varphi_X \cos\chi \dfrac{\sin 2\theta\cos\varphi_X}{\sqrt{1 - \sin^2\theta\cos^2\varphi_X}} \\ -0.25(p_{13} - p_{11})\sin\chi\sin 2\varphi_X \dfrac{\sin^2\theta\sin 2\varphi_X}{\sqrt{1 - \sin^2\theta\cos^2\varphi_X}} \\ -p_{44}\cos 2\varphi_X \sin\chi\sqrt{1 - \sin^2\theta\cos^2\varphi_X} \end{array} \right\}$$

$$\times \frac{\cos(\theta + \gamma)}{\sqrt{\cos^2(\theta + \gamma) + \sin^2(\theta + \gamma)\sin^2\varphi_X}}$$

The errors present in Eqs. (24)–(29) of Ref. [1] have led to some errors in the corresponding results and their interpretation. The corrected versions of Fig. 2 to Fig. 7 and the appropriate figure captions in Ref. [1] are as follows:
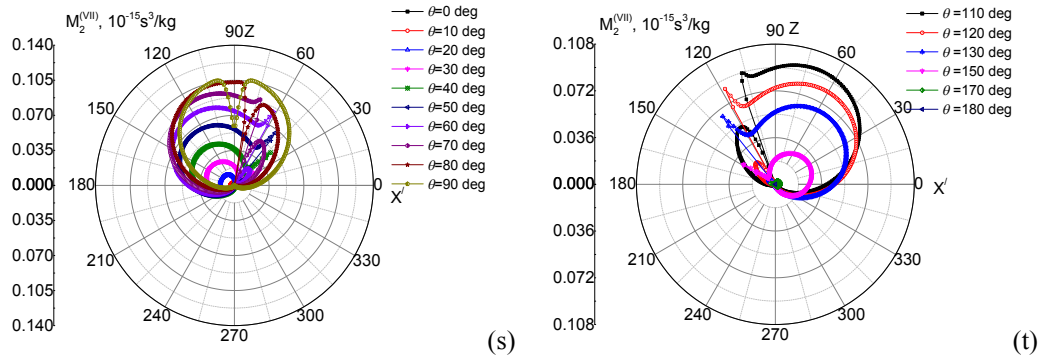

(a)   (b)

(c)

(d)

(e)

(f)

(g)

(h)

(i)

(j)

Ukr. J. Phys. Opt. 2016, Volume 17, Issue 4

151

(k)

(l)

(m)

(n)

(o)

(p)

(q)

(r)

152

Ukr. J. Phys. Opt. 2016, Volume 17, Issue 4

(s)

(t)
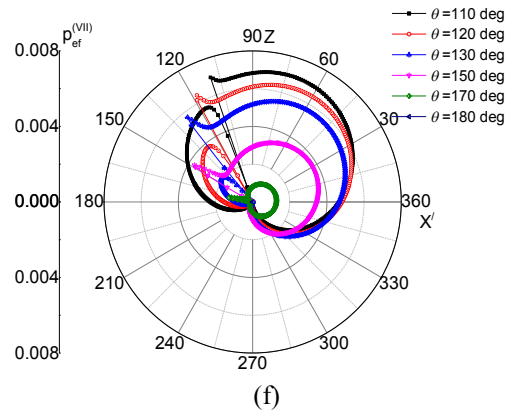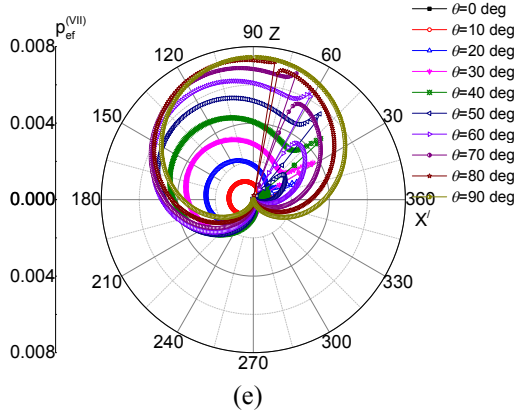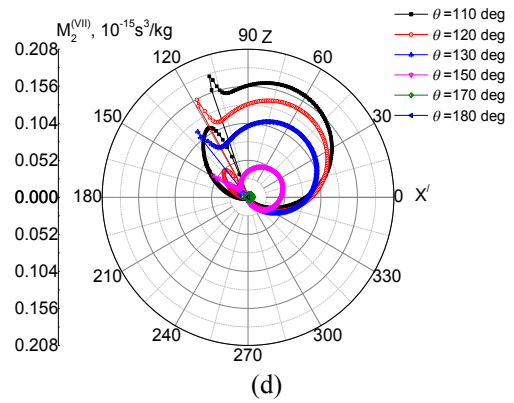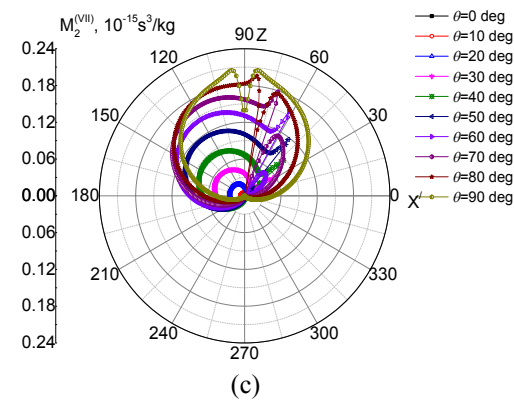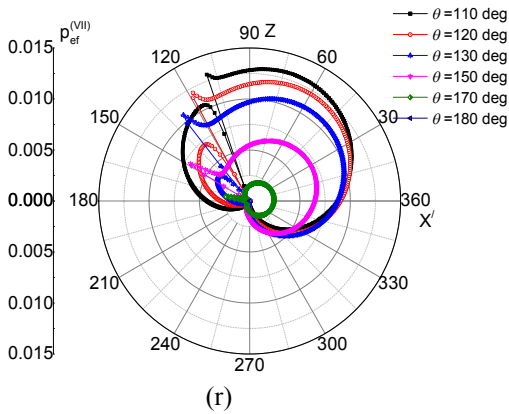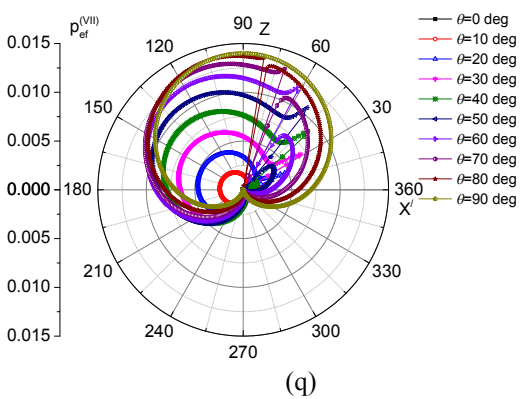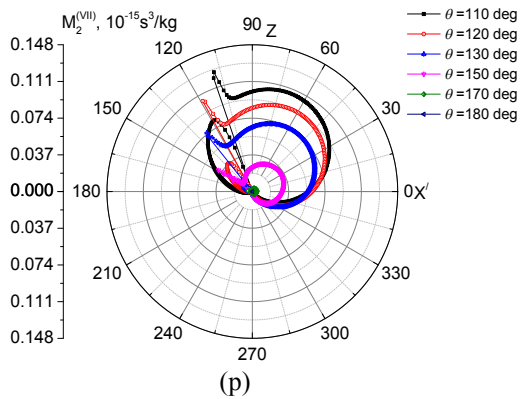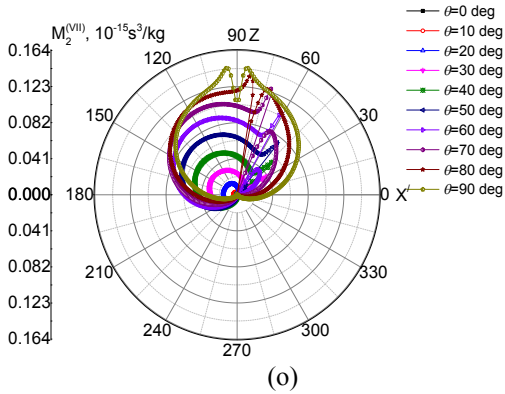
Fig. 2. Dependences of EOC (a, b, e, f, i, j, m, n, q, r) and AOFM (c, d, g, h, k, l, o, p, s, t) on the angle $\theta + \gamma$ at different incidence angles θ and for different orientations of the interaction plane $X'Z$ given by the angle φ_Z : φ_Z = 20 (a, b, c, d), 40 (e, f, g, h), 50 (i, j, k, l), 60 (m, n, o, p) and 80 deg (q, r, s, t). All the figures are associated with the type VII of AO interactions, i.e. the interactions with the longitudinal acoustic wave QL.
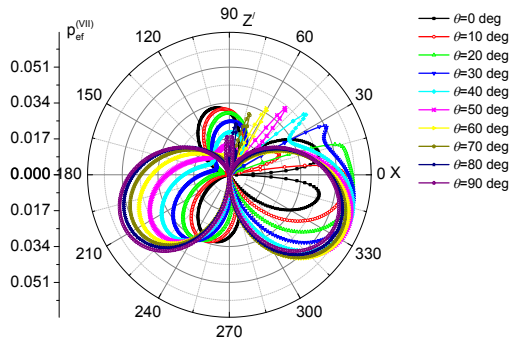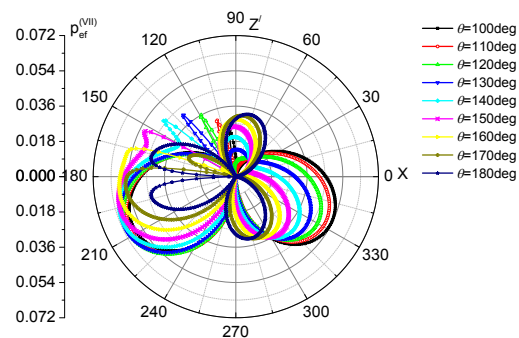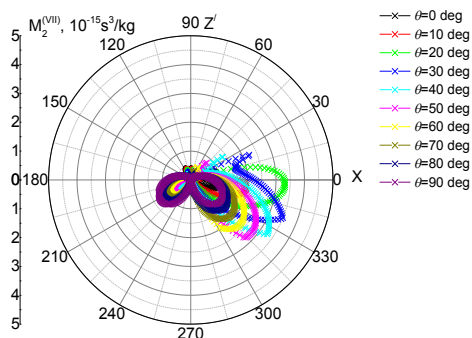

(a)

(b)

(c)

(d)

(e)

(f)

(g)

(h)

(i)

(j)

(k)

(l)

(m)

(n)

154

Ukr. J. Phys. Opt. 2016, Volume 17, Issue 4

(o)

(p)
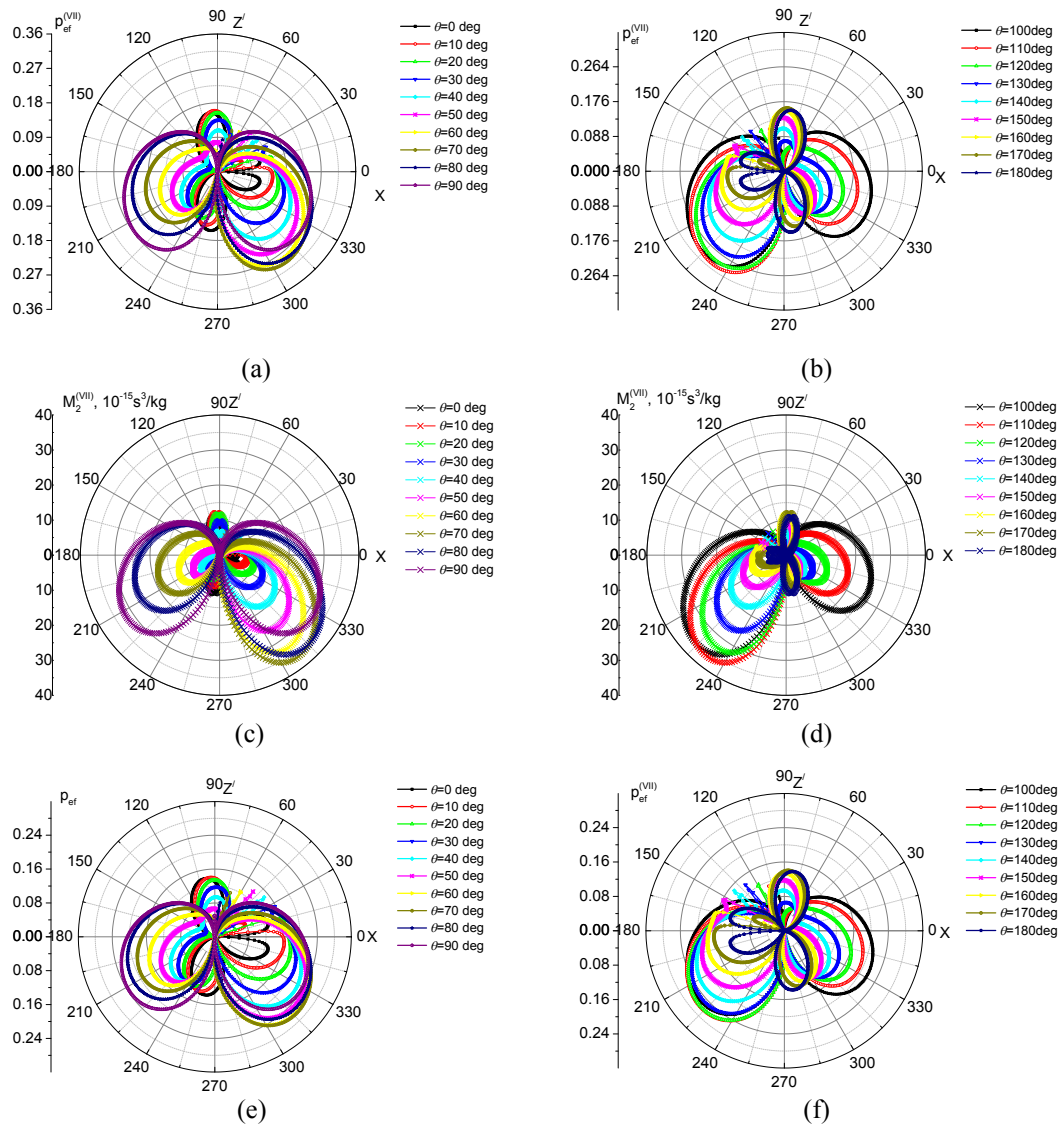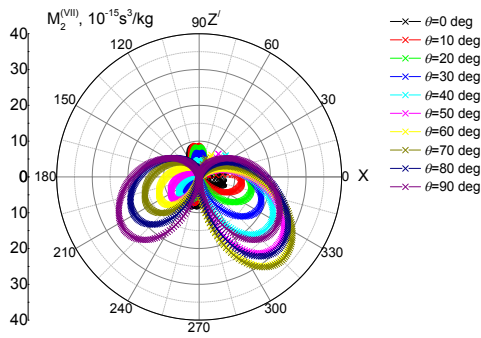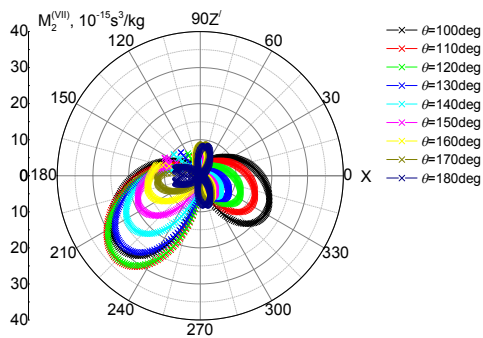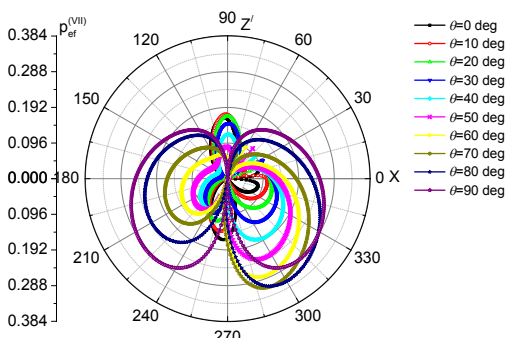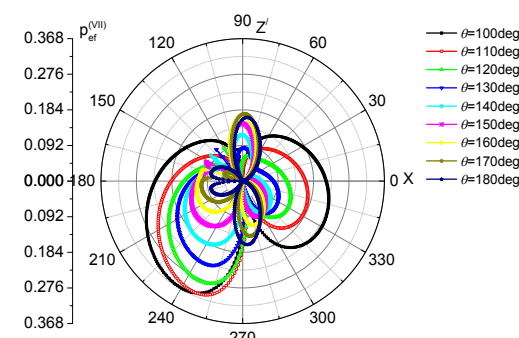
Fig. 3. Dependences of EOC (a, b, e, f, i, j, m, n) and AOFM (c, d, g, h, k, l, o, p) on the angle $\theta + \gamma$ at different incidence angles θ and for different orientations of the interaction plane XZ' given by the angle φ_X: φ_X = 30 (a, b, c, d), 40 (e, f, g, h), 80 (i, j, k, l) and 160 deg (m, n, o, p). All the figures are associated with the type VII of AO interactions, i.e. the interaction with the longitudinal acoustic wave QL.
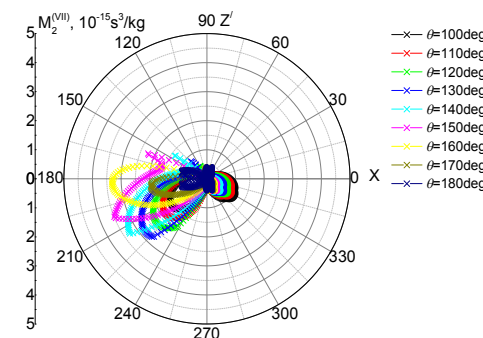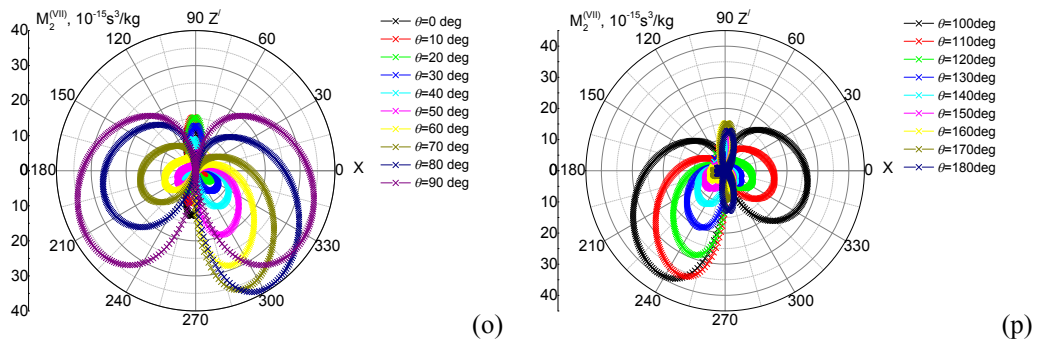

(a)

(b)

(c)

(d)

(e)

(f)

(g)

(h)

(i)

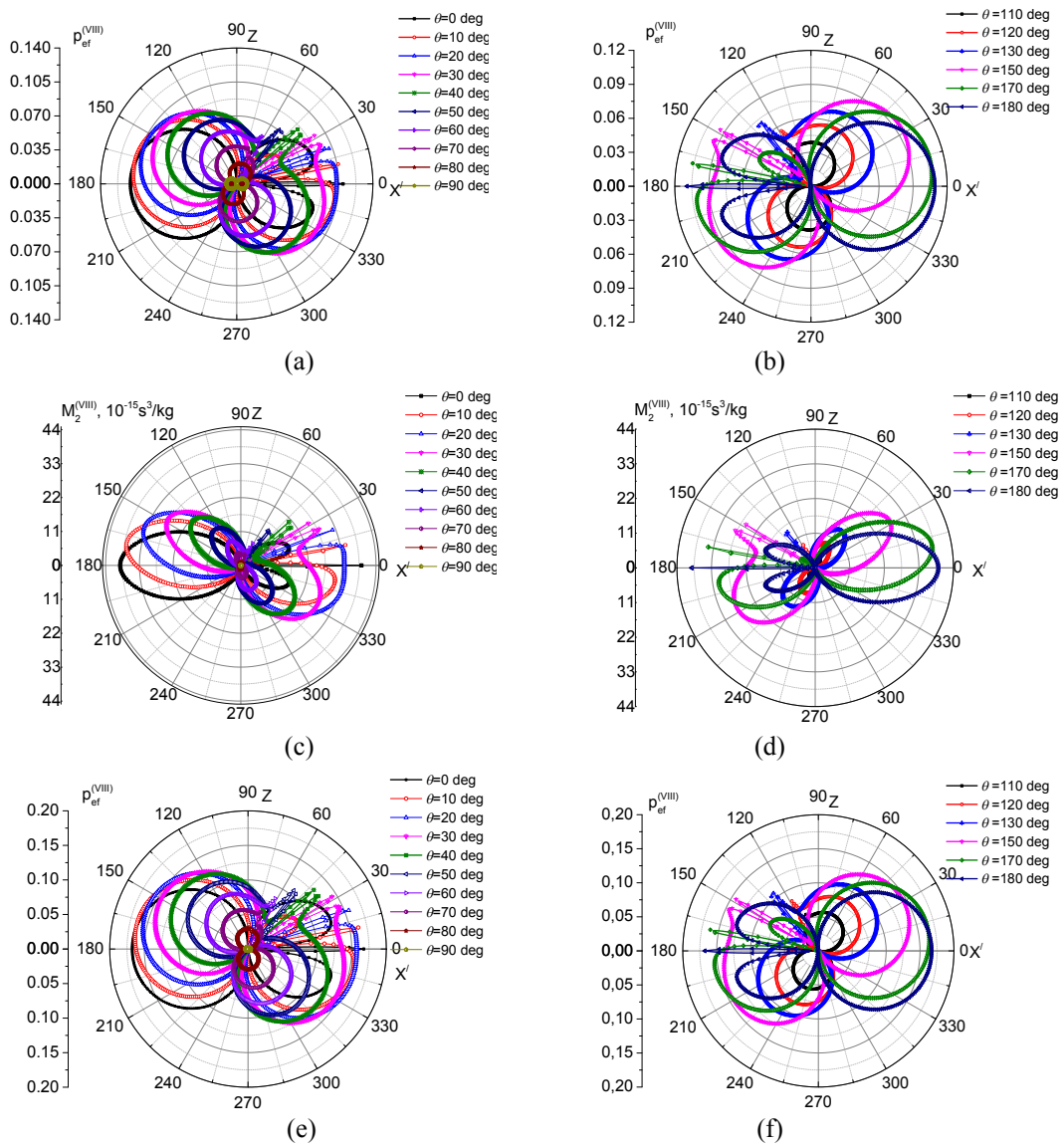(j)

(k)

(l)

(m)
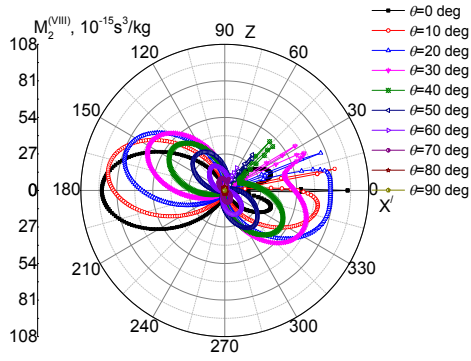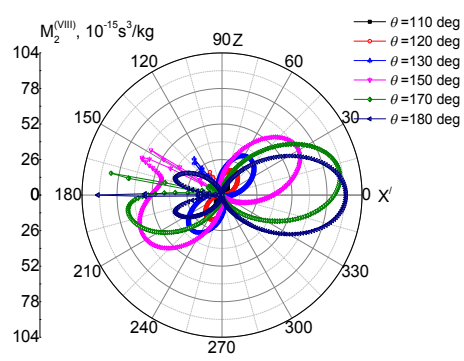

(n)

(o)

(p)
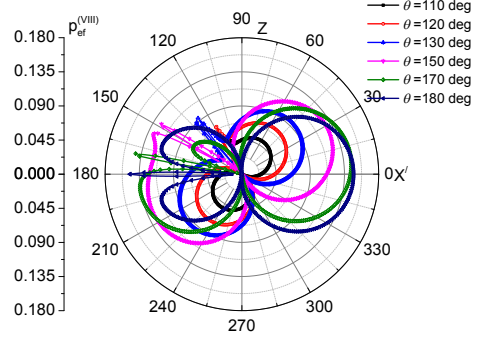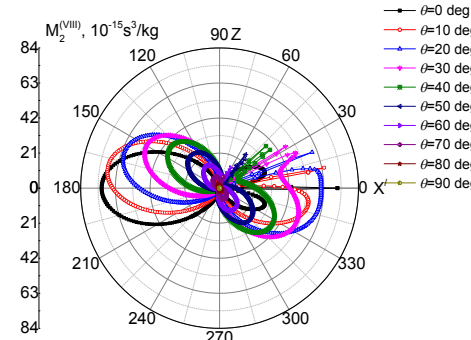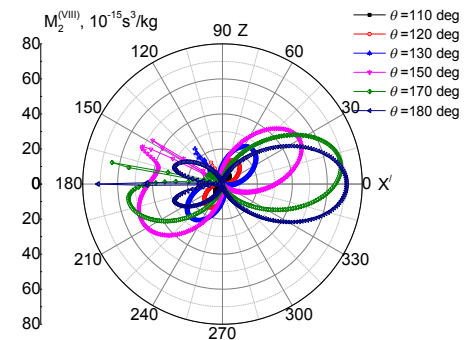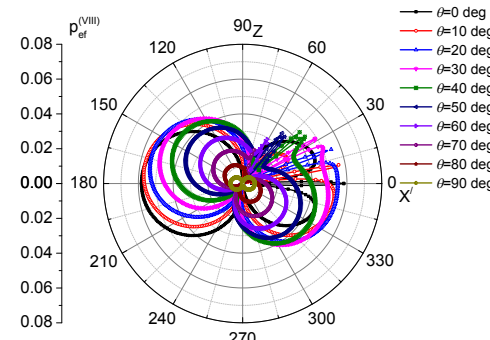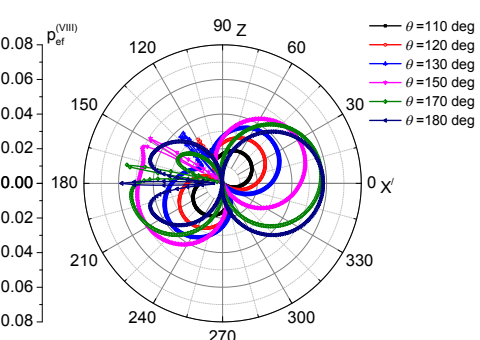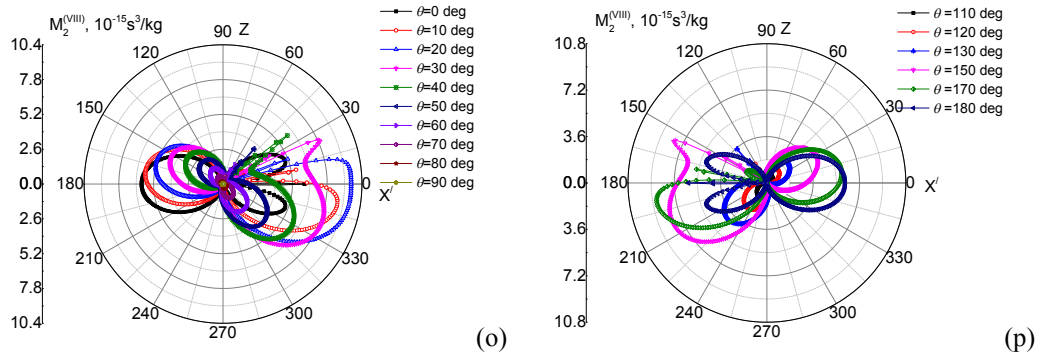
Fig. 4. Dependences of EOC (a, b, e, f, i, j, m, n, q, r) and AOFM (c, d, g, h, k, l, o, p, s, t) on the angle $\theta + \gamma$ at different incidence angles θ and for different orientations of the interaction plane $X'Z$ given by the angle φ_Z: $\varphi_Z = 20$ (a, b, c, d), 40 (e, f, g, h), 60 (i, j, k, l) and 80 (m, n, o, p). All the figures are associated with the type VIII of AO interactions, i.e. the interaction with the transverse acoustic wave $v_{13} = v_{QT_1}$.
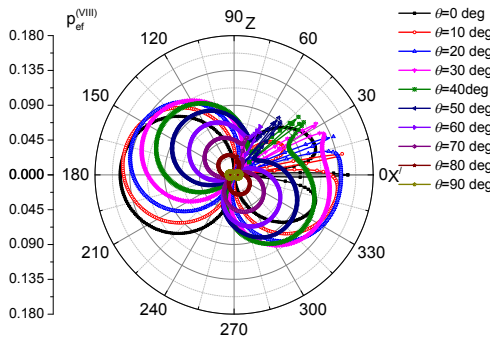

(a)

(b)

(c)

(d)

(e)

(f)

(g)

(h)

(i)

(j)

(k)

(l)

(m)

(n)

(o)

(p)

(q)

(r)

(s)

(t)
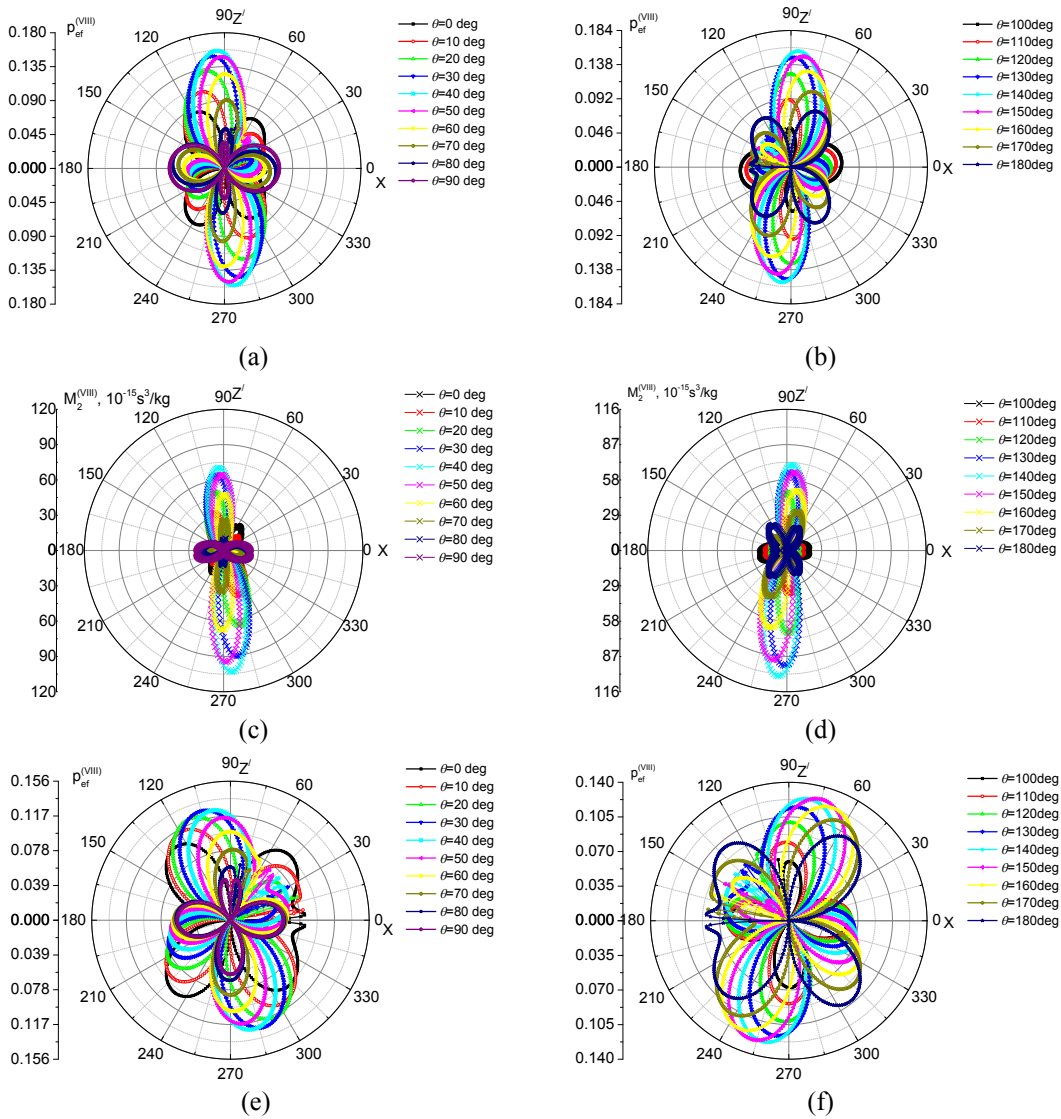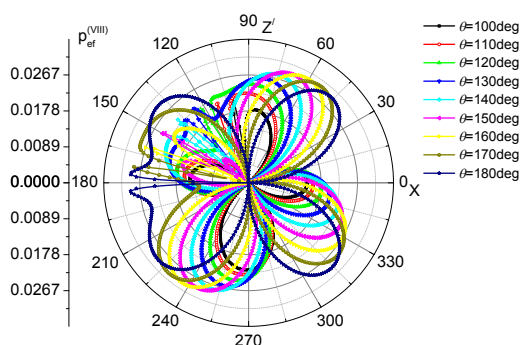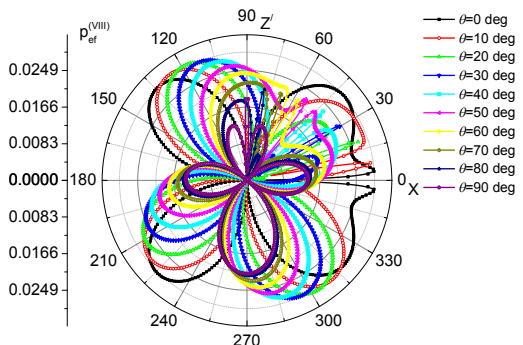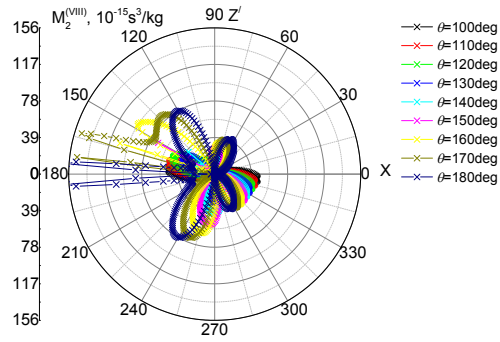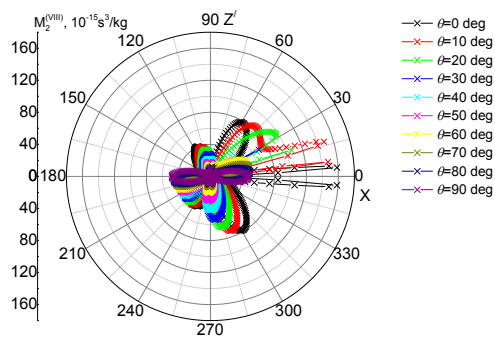
Fig. 5. Dependences of EOC (a, b, e, f, i, j, m, n, q, r) and AOFM (c, d, g, h, k, l, o, p, s, t) on the angle $\theta + \gamma$ at different incidence angles θ and for different orientations of the interaction plane XZ' given by the angle φ_X : φ_X = 20 (a, b, c, d), 40 (e, f, g, h), 60 (i, j, k, l), 80 (m, n, o, p) and 120 deg (q, r, s, t).All the figures are associated with the type VIII of AO interactions, i.e. the interaction with the transverse acoustic wave $v_{13} = v_{QT_1}$.

(a)

(b)

(c)

(d)

(e)

(f)

(g)

(h)

(i)

(j)

(k)

(l)

(m)

(n)

(o)

(p)

(q)

(r)

Ukr. J. Phys. Opt. 2016, Volume 17, Issue 4

161

(s)

(t)
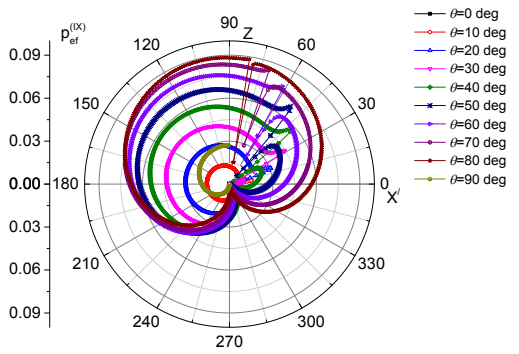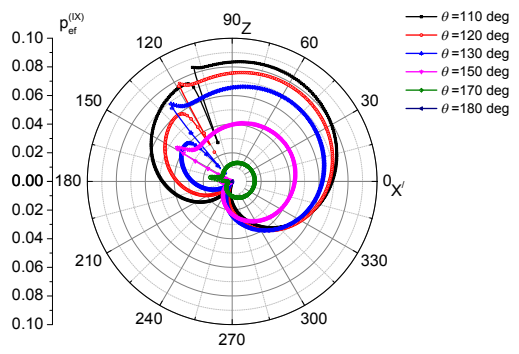
Fig. 6. Dependences of EOC (a, b, e, f, i, j, m, n, q, r) and AOFM (c, d, g, h, k, l, o, p, s, t) on the angle $\theta + \gamma$ at different incidence angles θ and for different orientations of the interaction plane $X'Z$ given by the angle φ_Z: φ_Z = 0 (a, b, c, d), 20 (e, f, g, h), 45 (i, j, k, l), 60 (m, n, o, p) and 90 deg (q, r, s, t). All the figures are associated with the type IX of AO interactions, i.e. the interaction with the transverse acoustic wave $v_{12} = v_{QT_2}$.

(a)

(b)

(c)

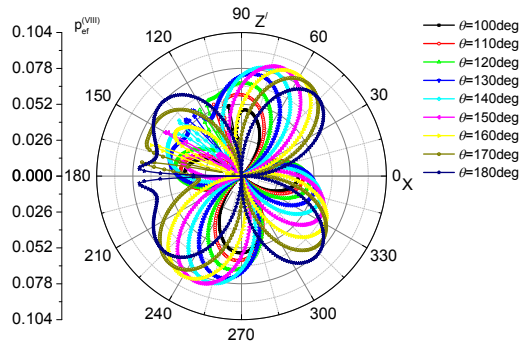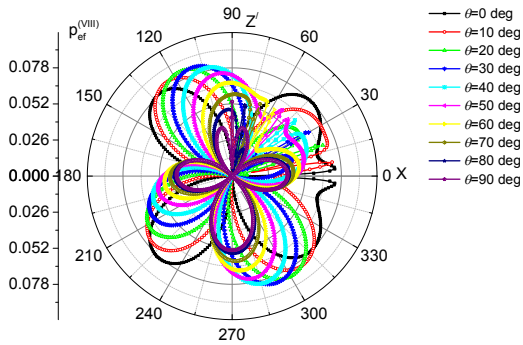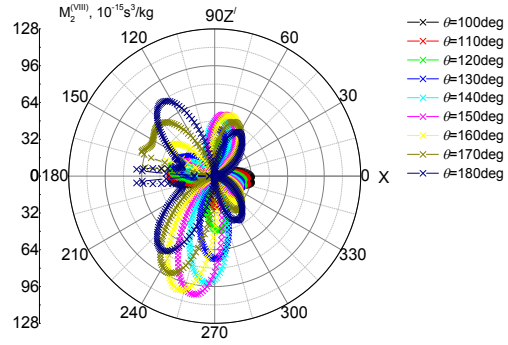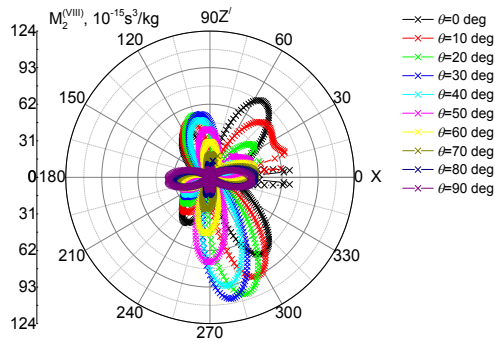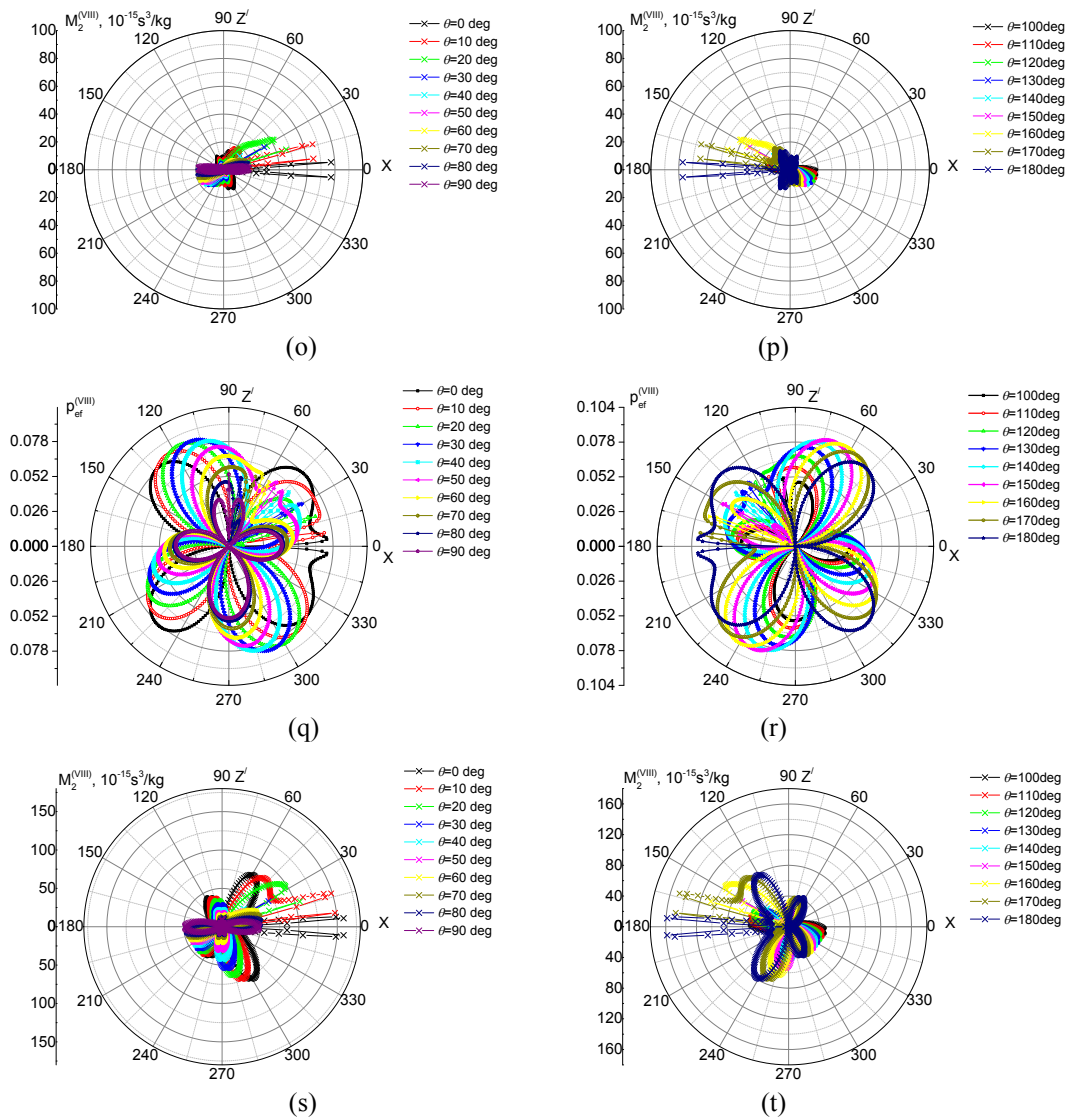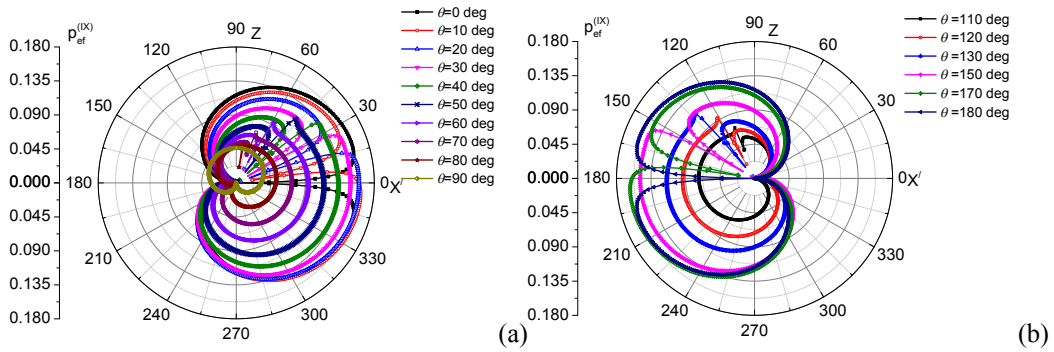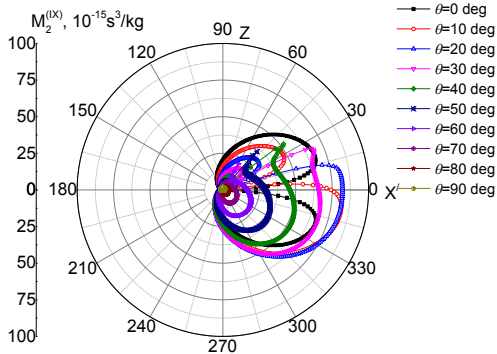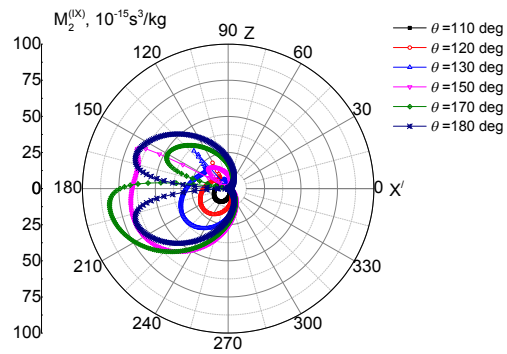(d)

(e)

(f)

(g)

(h)

(i)

(j)

(k)

(l)

(m)

(n)
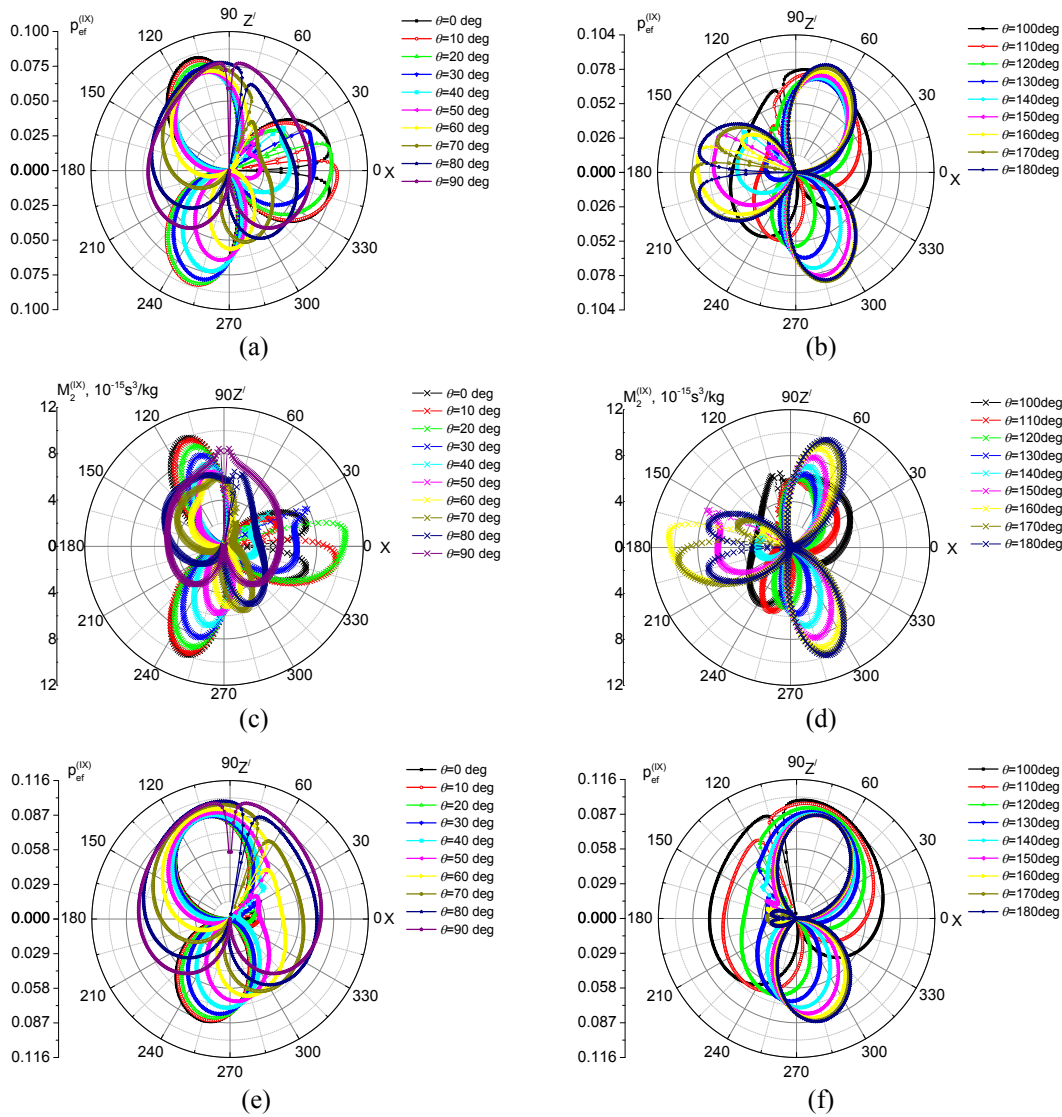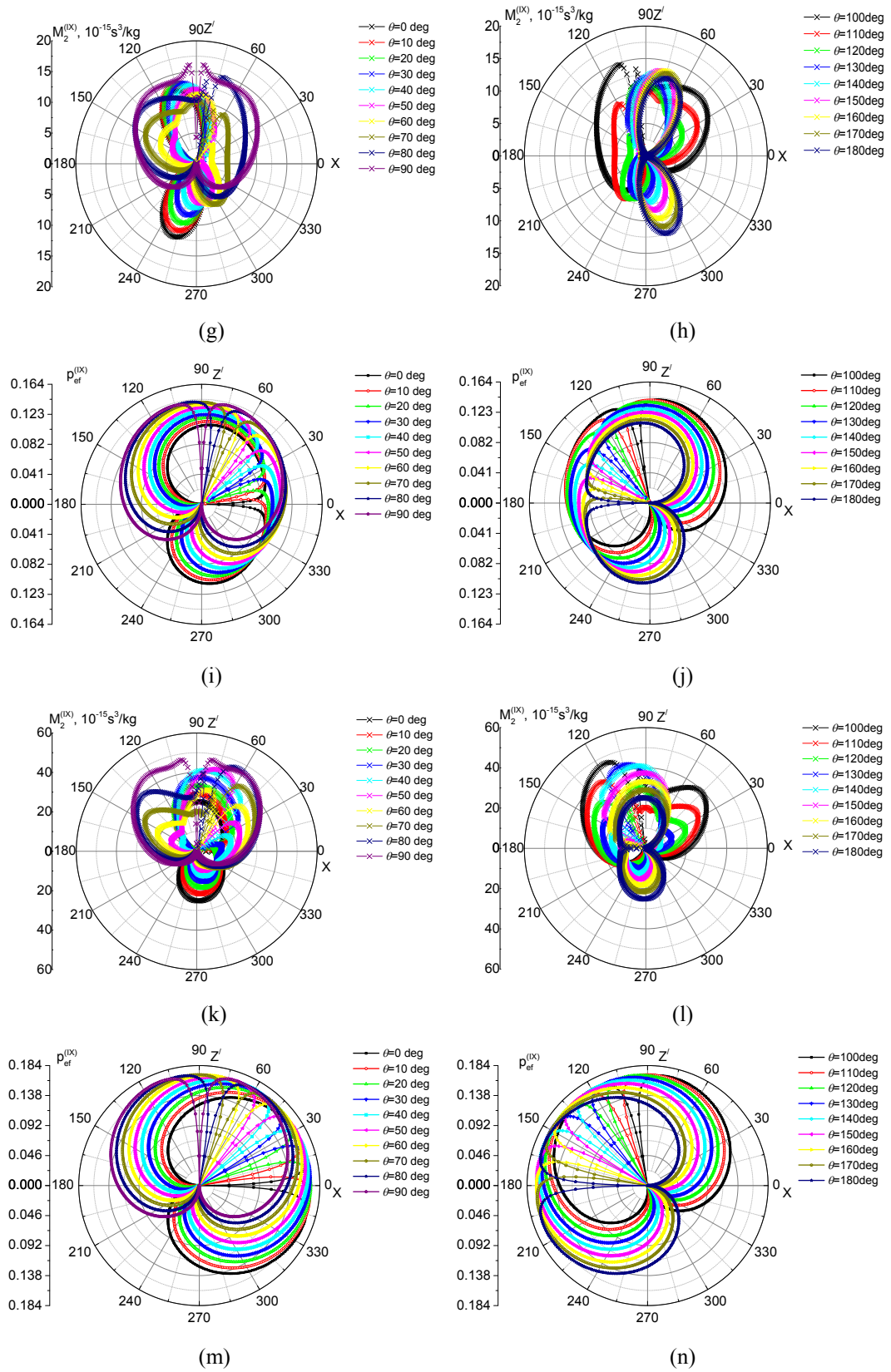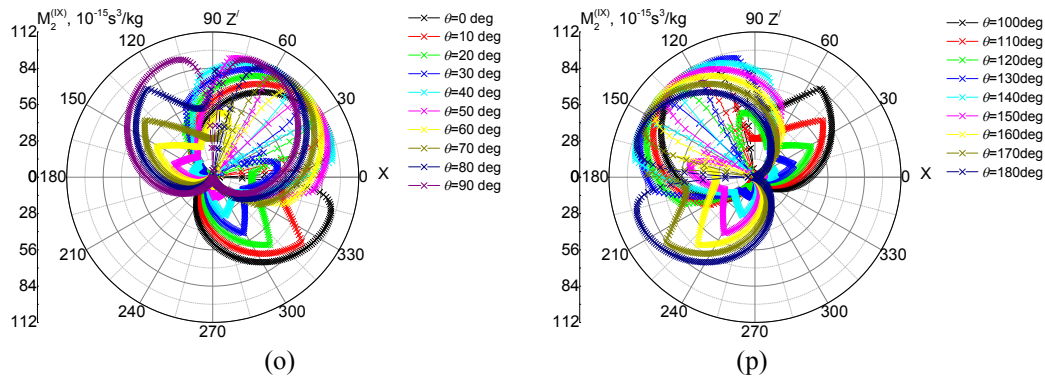
Fig. 7. Dependences of EOC (a, b, e, f, i, j, m, n) and AOFM (c, d, g, h, k, l, o, p) on the angle $\theta + \gamma$ at different incidence angles θ and for different orientations of the interaction plane XZ' given by the angle φ_X: φ_X = 30 (a, b, c, d), 40 (e, f, g, h), 60 (i, j, k, l) and 90 deg (m, n, o, p). All the figures are associated with the type IX of AO interactions, i.e. the interaction with the transverse acoustic wave $v_{12} = v_{QT_2}$.
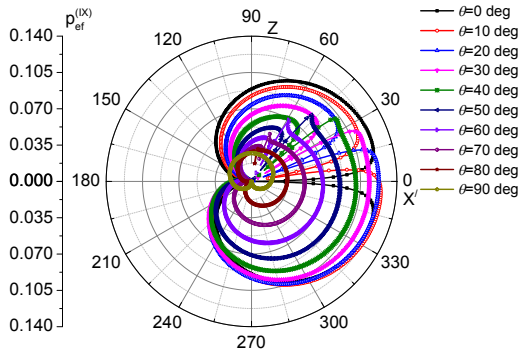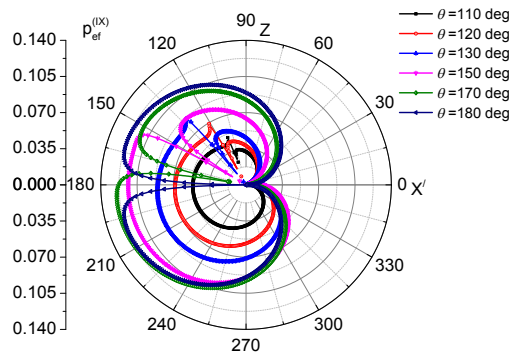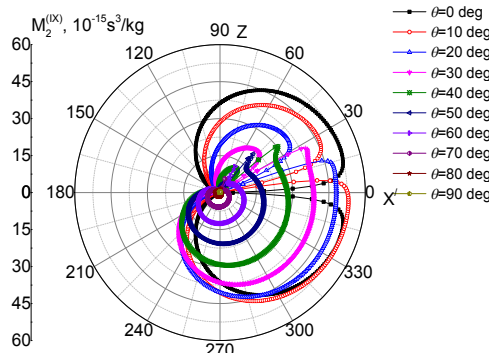
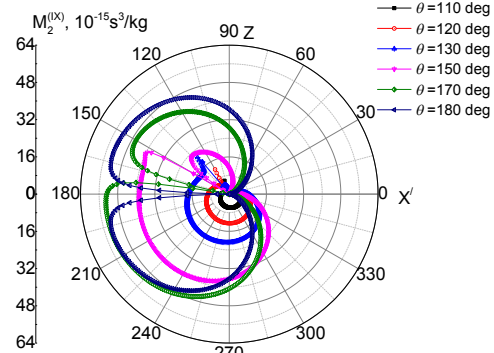Moreover, Section 3 "Results and discussion" and Section 4 "Conclusions" need to be partly rewritten as follows.

3. Results and discussion

(Beginning from the first sentence immediately below Eq. (30)). Now we consider the dependences of the EOC and the AOFM M_2 on the angle $\theta + \gamma$ at different angles of incidence θ and at different orientations of the interaction planes $X'Z$ and XZ', which are defined respectively by the angles φ_Z and φ_X. Let us analyze the interaction type VII that corresponds to the AO interactions with the longitudinal acoustic wave. As seen from Fig. 2 and Fig. 3, both the EOC and the AOFM reveal considerable anisotropy associated with the AO interactions occurring in the ZX plane. The exact size of the anisotropy depends on the incidence angle θ and the sum of angles $\theta + \gamma$.

The maximal AOFM value for the interaction type VII ($39.3 \times 10^{-15} \text{s}^3/\text{kg}$) is reached when the interaction plane is rotated around the X axis by the angle $\varphi_X = 160$ deg. The angle of incidence of the optical wave is equal to 80 deg and the angle $\theta + \gamma$ to 303 deg (see Fig. 3o). Thus, the diffraction angle $\gamma = 223$ deg turns out to be close to the value 180 deg, which defines a so-called 'reflection' diffraction type. It is worth noting that the EOC and the AOFM become zero whenever the interaction planes coincide with the principal crystallographic planes. Among the geometries of collinear diffraction linked to the interaction type VII, the maximal AOFM ($8.4 \times 10^{-15} \text{s}^3/\text{kg}$) is reached in the interac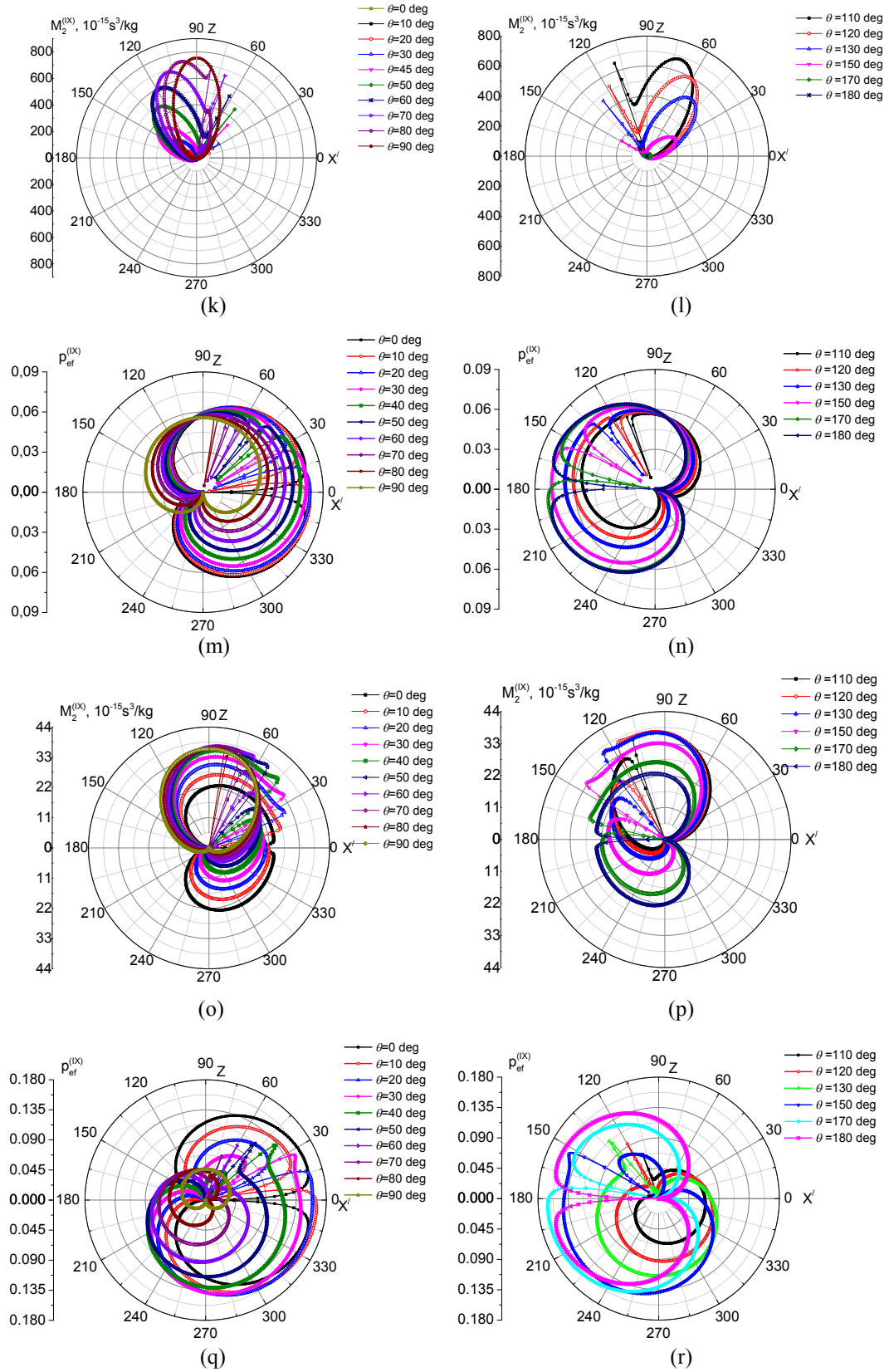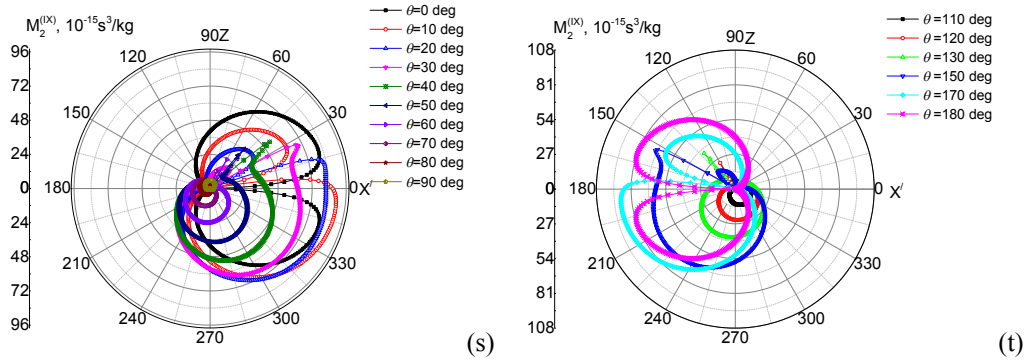tion plane rotated by 40 deg around the X axis, at the incidence angles $\theta = 50$ and 130 deg for the optical wave and the diffraction angle $\gamma = 0$ deg (see Fig. 3g).

If the type VIII of AO interactions in the plane XZ' is dealt with (see Fig. 4 and Fig. 5), the maximal AOFM ($158.5 \times 10^{-15} \text{s}^3/\text{kg}$) is reached when the interaction occurs in the plane rotated by 60 deg around the X axis (see Fig. 5k). Then the incident optical wave propagates along the X axis and the diffracted wave at the angle ± 4 deg with respect to the same axis. The maximal AOFM for the collinear diffraction of the interaction type VIII ($92.2 \times 10^{-15} \text{s}^3/\text{kg}$) takes place in the interaction plane rotated around the Z axis by the angle 40 deg (see Fig. 4g) at the incidence angles equal to $\theta = 0$ and 180 deg.

As for the type IX of interactions with the transverse acoustic wave v_{12} (see Fig. 6 and Fig. 7), the AOFM maximum ($\sim 750 \times 10^{-15}$ s^3/kg) is reached in the plane rotated by $\varphi_Z = 45$ deg (see Fig. 6k). The incident and diffracted waves belong to the plane (110) and propagate close to the optic axis. For the collinear AO interactions, the maximal M_2 value (29.9×10^{-15} s^3/kg) is peculiar for the same interaction plane, when both the optical and the acoustic waves propagate along the direction inclined by the angle 20 deg with respect to the X' axis.

Table 1 depicts the AOFM values calculated for different types of anisotropic AO interactions in TeO$_2$ crystals, using the technique described above. One can see that the maximal AOFM is reached for the type IX of AO interactions with the slowest transverse acoustic wave QT$_2$, which propagates along the bisector of the X and Y axes and is polarized parallel to $[\bar{1}10]$. The AOFM for this case is equal to $\sim 750.0 \times 10^{-15}$ s^3/kg.

Now it is interesting to combine all the results derived in the work [2] for the isotropic diffraction with the data obtained in the present study for the anisotropic diffraction in TeO$_2$ crystals. Let the polarization states of the optical waves correspond to the eigenstates. The highest AOFM value is peculiar for the isotropic interaction of the type III (1143.8×10^{-15} s^3/kg). It is achieved for the AO interactions with the same slow acoustic wave that propagates with the velocity 612 m/s. The increase in the AOFM from 750.0×10^{-15} s^3/kg to 1143.8×10^{-15} s^3/kg observed when passing from anisotropic to isotropic diffraction is provided by moderate increases in both the EOC and the refractive index.

Notice that the AOFM of TeO$_2$ crystals can still be slightly increased (up to 1200×10^{-15} s^3/kg) when the incident optical wave is circularly polarized and propagates almost parallel to the optic axis [3]. However, the interaction conditions for the latter case are strongly limited by severe requirements for the propagation directions of the incident and diffracted waves. Namely, these waves have to propagate along the directions in which the eigenwaves are highly elliptic and a small linear birefringence still exists. These conditions are satisfied only when the both optical waves propagate very close to the optic axis.

Table 1. Maximal AOFM values M_2 calculated for different types of anisotropic AO interactions in TeO$_2$ crystals, and descriptions of the corresponding geometries.

Type of AO interaction	Angle $\varphi_{Z,X}$ of orientation of the interaction plane	Acoustic wave velocity, m/s	Type of acoustic wave	Directions of acoustic wave propagation and polarization	AOFM M_2, 10^{-15} s^3/kg
VII	$\varphi_X = 160$ deg	4086	QL	$\chi = -79.1$ deg, parallel to the wave vector	39.3
VIII	$\varphi_X = 60$ deg	2577	QT$_1$	$\chi = 135$ deg, belong to the interaction plane	158.5
IX	$\varphi_Z = 45$ deg	612	QT$_2$	$[110]$, $[\bar{1}10]$	750.0

Let us compare the efficiencies of the collinear AO diffractions in TeO$_2$ for different types of anisotropic interactions. As seen from Table 2, the AOFM maximum for the collinear AO interactions is achieved for the interaction type VIII, when both of the optical waves and the acoustic wave QT$_1$ propagate in the plane(001) along the direction inclined by 40 deg with respect to the X axis. Then the AOFM equals to 92.2×10^{-15} s^3/kg. Nonetheless, the AOFM for the collinear interaction with the longitudinal acoustic wave propagating along [011] is also high enough (39.3×10^{-15} s^3/kg).

Table 2. Maximal AOFM values M_2 calculated for different types of collinear anisotropic AO interactions in TeO$_2$ crystals, and descriptions of the corresponding geometries.

Type of AO interaction	Angle $\varphi_{Z,X}$ of orientation of the interaction plane	Acoustic wave velocity, m/s	Type of acoustic wave	Direction of acoustic wave propagation and polarization	AOFM M_2, 10^{-15} s^3/kg
VII	$\varphi_X = 40$ deg	3866	QL	$\chi = 50$ and 130 deg, parallel to the wave vector	8.4
VIII	$\varphi_Z = 40$ deg	2018	QT$_1$	$\chi = 0$ and 180 deg, parallel to the wave vector	92.2
IX	$\varphi_Z = 45$ deg	903	QT$_2$	$\chi = 20$ deg, parallel to the wave vector	29.9

4. Conclusions

(*Beginning from the second paragraph*). We have found that the highest AOFM value for TeO$_2$ crystals (1143.8×10^{-15} s^3/kg) can be reached when the linearly polarized optical eigenwaves interact isotropically with the transverse acoustic wave QT$_1$. This AO diffraction belongs to the interaction type III. We have also demonstrated that the AOFM for the cases of collinear AO diffraction is characterized by sharp angular peaks and dips. The maximal AOFM value for the collinear diffraction is reached at the AO interaction with the acoustic wave QT$_2$ (the interaction type IX). The corresponding wave QT$_2$ should propagate along the direction [110] and be polarized along [$\bar{1}$10]. In this case, the AOFM is equal to $\sim 750 \times 10^{-15}$ s^3/kg. The maximal AOFM value for the collinear diffraction is equal to 92.2×10^{-15} s^3/kg.

References

1. Mys O., Kostyrko M., Krupych O. and Vlokh R, 2015.Anisotropy of acoustooptic figure of merit for TeO$_2$ crystals. 2. Anisotropic diffraction. Ukr. J. Phys. Opt. **16**: 38–60.
2. Mys O, Kostyrko M, Smyk M, Krupych O and Vlokh R, 2014. Anisotropy of acoustooptic figure of merit for TeO$_2$ crystals. 1. Isotropic diffraction. Ukr. J. Phys. Opt. **15**: 132–154.
3. Yano T and Watanabe A, 1974. Acousto-optic figure of merit of TeO$_2$ for circularly polarized light. J. Appl. Phys. **45**: 1243–1245.

Анотація. *Виправлено помилки, знайдені нами в нещодавньому аналізі анізотропії коефіцієнта акустооптичної якості в кристалах TeO$_2$ [Mys O. et al., 2015. Ukr. J. Phys. Opt. 16: 38–60].*